Computation of Amplification Factor of the Mechanical Power Amplifier for Different Rope Materials

Okundaye Osama Samuel
Department of Mechanical Engineering
Edo State Polytechnic, Usen, Edo State, Nigeria

Abstract

Engineering applications often must control a substantial output load using a relatively low control force. Mechanical power amplifiers come into play to address this requirement, providing rapid response and efficient power transfer. In this study, we focus on computing the amplification factor of a mechanical power amplifier for various rope materials, including leather, woven cotton, and steel. The experimental analysis involves a capstan mechanism, where a rope is wound around a motor-driven drum. The drum continuously rotates, but torque transmission occurs only when the input shaft constricts the drum. Our investigation aims to determine the amplification factor for different rope types. The results reveal that leather contact is optimal when the number of turns is approximately two, yielding an amplification factor of 2.23. Woven cotton contact achieves an amplification factor of 1.867. while steel contact provides an amplification factor of 1.32. Interestingly, leather outperforms woven cotton and steel in terms of power amplification. These findings align well with experimental measurements and demonstrate the mechanical power amplifier's favorable performance.

Keywords: computation factor, mechanical power amplifier, capstan, rope materials

Introduction

The amplification factor of an optical amplifier is the factor that amplifies the input power. The performance of laser amplifiers is influenced by factors such as the characteristics of the laser gain medium, its excitation level, optical wavelength, and beam polarization. The length of the nonlinear crystal, pump intensity, beam diameters, and various other parameters influence the performance of optical parametric amplifiers. An electrical amplifier specifically made to boost the power of a signal fed into it is called a power amplifier (Bienert et al., 2022; Choi, 2023; Jeong et al., 2023; Wang et al., 2022). The input signal is amplified to a degree where it can power several output devices. Depending on their changes to the incoming signal, amplifiers can be categorized as current, voltage, or power amplifiers. In this paper, power amplifiers are examined from the perspective of mechanics. Mechanical power amplifiers are electronic devices that are built on the Capstan architecture. These amplifiers aim to increase the strength of an electrical signal. Utilizing motorized drum slides to pick up the slack on the free end of the rope, the capstan is a basic mechanical amplifier. The capstan is employed when the user is required to lift or pull anything heavier than they can handle. The twist count and coefficient of friction of the rope determine how much force is required on the free end to lift the load. By employing bands coupled to an input shaft and arm, the power amplifier may offer an output in both directions and accurate angular positioning (Thokale, 2016).

A mechanical device called a capstan mechanical amplifier is characterized by a drum and gear configuration and a single electrical motor powered by electrical energy. In most cases, capstans are utilized for lifting or pulling big objects with the assistance of winches. According to Starkey and Williams (2011), a capstan can dynamically magnify the input by altering the strain that is placed on the cable based on the input. These devices enhance the power share partially supplied to the drum and change its control force. Power can be provided in both directions between the input and output shafts by mounting two rotating drums in a back-to-back configuration (Gawande, 2018). Conventional electrical, hydraulic, and pneumatic transducers can all be replaced by this revolutionary device. Because of this, the chance of cumulative inaccuracy brought about by using transducers is reduced. When a flexible rope line is looped around a cylinder, the Capstan principle establishes a relationship between the holding force and the load force (Baser & Ilhan Konukseven, 2010; Li et al., 2022; Qi et al., 2018; Schumann et al., 2022). The friction between the rope and the drum is caused by applying force in the direction of rotation. The force exerted by the user will be amplified due to the generated friction, which will act in the same direction as the pull.

In a general sense, the goal of the capstan is to produce a suitable amount of friction force between the drum and the rope to allow the rope to travel at the same pace as the drum. Most lifting and winching activities should not cause any slippage. It is possible that the utilization of the capstan could be classified as static because static friction is produced when the rope rubs against the capstan in this manner. On the other hand, if the rope is allowed to slide around the drum, there will be kinetic friction, and the system can be characterized as dynamic (Paynter, 2002).

Researchers have investigated different alterations in the Capstan amplifiers. Thomas et al. (2012) studied the characterization of a continuously variable linear force amplifier based on Capstan's theory, employing an elastic wire to enable a control actuator to declutch by releasing tension. The study shows that using a system of distributed capstan amplifiers powered by a central torque source, with cable engagement controlled by lightweight, low-torque actuators, could decrease the weight of distal actuators and enhance agility in robotic tasks. Hu et al. (2012) created a displacement amplifier to enhance the accuracy and resolution of an extensometer for measuring strain in high-temperature components. The results confirm the accuracy of the amplification ratio equation and show that the extensometer rods can exert the loading force produced by the flexure hinge's torque moment. Hu et al. (2016) developed an electrostatic sensing system to detect the lateral vibration of power transmission belts continuously and without physical touch. The results indicate that the belt vibrates at distinct modal frequencies that rise with axial speed. A shorter distance between the electrode and the belt allows for detecting higher-order vibration modes. However, it also causes significant signal distortion, resulting in higher-order harmonics.

Shahosseini and Najafi (2014) detailed the design, optimization, and testing outcomes of a mechanical amplifier connected to an electromagnetic energy harvester to produce electricity from small-amplitude (1 mm) and low-frequency (5 Hz) vibrations despite significant static displacements. The study shows that a complete electromagnetic energy harvester with this mechanical amplifier produces a high-power density of 170 W/cm3 and a 16-fold increase in output power (30 mW compared to 1.9 mW without the amplifier at 5 Hz). The capstan amplifier typically involves a rope coiled around a drum to enhance the amplification of a weight connected to one end of the rope by interacting with the tension. The likelihood of the rope getting tangled increases as more turns are added. Increased tension in the cord while binding enables the rope to securely fasten to the drum, causing the kinetic friction coefficient to surpass the static friction coefficient.

A mechanical power amplifier has a comparatively fast response time. Its continuously rotating drums allow instantaneous access to electricity. Pneumatic, hydraulic, and electrical systems need transducers to convert signals from one energy type to another when they are used for position control applications. This remains true even in the event of continuously running power sources. However, the mechanical power amplifier makes direct perception of the controlled motion possible. This study looks at assessing a power amplifier prototype's performance using the amplification factor and design optimization for several turns of rope material. The study's main goal was to calculate the amplification factor of the Capstan model mechanical power amplifier for different rope materials.

Experimental Set-Up and Construction

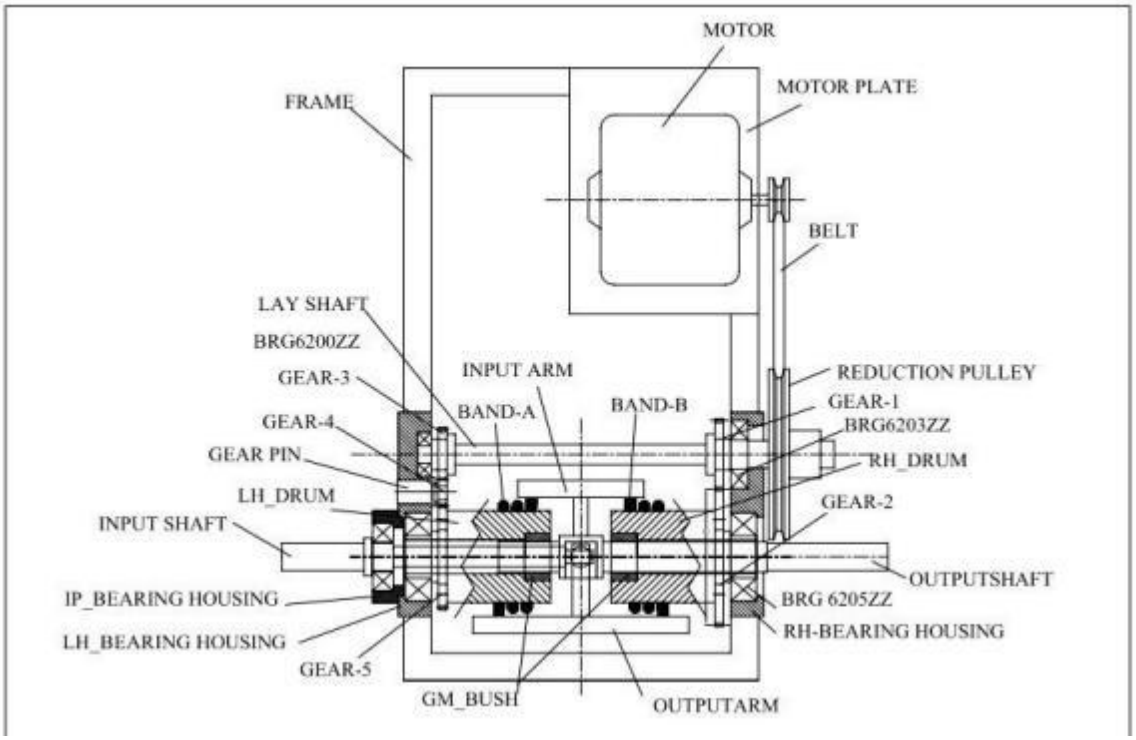

Fig. (1). Experimental set-up for capstan power amplifier.

The production overshot is halted by the drum-tightening band B around it. The slip persists until the loose end tightens. The coefficient of friction (COF) and the number of rotations impact the force required at the free end to raise the load. The power amplifier accurately adjusts the orientation of connecting bands A and B to produce an output in both directions. When the input shaft is spun clockwise (CW), the input arm takes up the slack in band A and secures it to its drum. Band A's locked end is attached to the output arm, transmitting the clockwise motion of the driven drum to the output shaft. When a flexible line is wrapped around a cylinder, the belt friction or capstan equation determines the holding and load forces relationship, such as with a bollard or winch.

A Capstan system relies on the holding force applied on one side to support a significantly larger loading force on the opposite side. Bands A and B are linked to an input shaft and arm through the power amplifier, which provides output directions and accurate angular positioning. When the input shaft is turned clockwise, the input arm tightens band A and secures it to its drum. Band A, when locked, transfers the clockwise rotation of the tail drum to the output shaft by connecting the load end of the band to the output arm. Consequently, band B becomes lethargic and stumbles over its drum. Band A slips on its drum when the input shaft stops rotating clockwise because the tension is no longer restricted. The output arm will tighten band B on the counterclockwise revolving drum and stop the shaft if it tries to rotate too quickly. The motor rotates Drum-B counterclockwise, causing the input shaft to move in the opposite direction. The diameter of the drums, the number of wraps on the bands on each drum, and the coefficient of

friction between the drum and band collectively influence the increased torque. Through the amplifier design indicated, input power applied to the input shaft is increased and transferred to the output shaft.

Fig. (2). The prototype of Capstan mechanical power amplifier

Table 1: Capstan mechanical power amplifier components.

1	Electrical Motor	The electrical motor has a variable speed range of 0 to 9500 rpm and has a 50-watt capacity. An electronic speed variator is used to control the speed. The motor's motor pulley provides the system's drive, and the reduction pulley is positioned on the layshaft.
2	Motor Selection	The power is transmitted to the input shaft of the amplifier using an open belt drive using two pulleys and a belt on a single-phase AC Motor with a 2 kg-cm Torque and 6000 rpm speed with 50-watt input power. The motor pulley diameter (25 mm), input shaft pulley diameter (100 mm), input speed (2100 rpm). Output speed at lay shaft (2100/4 =525), rpm Power ($2 \times \pi \times 2100 \times .20/60 = 43.98$ W).
3	Lay Shaft	Two ball bearings installed in a bearing housing support the layshaft, built of the material EN4, and have mechanical qualities. The layshaft carries the reduction pulley and a set of gears from the gear train at one end.
4	Gear Train Specification	Gear-1: 1. 5 modules, 18 teeth, and a 5mm face width Gear-2: 1. 20 teeth, 5 modules, and a 5mm face width Gear-3: 1. 5 modules, 40 teeth, and a 5mm face width Gear-4: 1. 5 modules, 32 teeth, and a 5mm face width. Gear-5: 1. 5 modules, 64 teeth, and a 5mm face width
5	LH and RH Drums	The output shaft is supported by a gunmetal bushing attached to the left and right-hand drums, located in bearings 6005ZZ and 6005ZZ, respectively, in the bearing housing. The band is coiled around the drums and connected to the input and output arms at its two ends, respectively.
6	Input and Output Arms	The input and output arms are connected to the input shaft and output shaft. The band wound on the drums is connected to these arms at their two ends.
7	Input Shaft	The input shaft has a ball bearing 6203zz installed on one end that is retained in the input shaft housing, and the input arm is attached to the other end.
8	Output Shaft	The output shaft is placed inside the load drums by gunmetal bush bearings. One end

		of the output shaft is hollow so the input shaft can pass through it.
9	Frame	The frame is the part of the power amplifier that holds it alltogether. The LH and RH bearing housings and the motor plate are welded to the frame.
10	Rope	The rope is made of cotton beads and has a diameter of 6 mm. The left band is wound around the left drum, and the right band is wound around the right drum. Both the input and output arms are attached to the ends of these bands.

Test Trials and Measurement

To conduct the trial, a dyno-brake pulley cord and weight pan are provided on the output shaft.

Input Data

1, Drive Motor < AC230 Volt - 0.5 Amp, 50 watt - 50 Hz, 200 to 9500 rpm
(TEFC Commutator Motor)

2. Select the leather material for the rope and wound *three* numbers of the turn-around corresponding drums. Then, trials are conducted by the following procedure.

Procedure

The motor started by shifting the electronic speed variator knob to allow the mechanism to run & stabilize at a certain speed (e.g., 1300 rpm). The weight in the weight pan was attached to the input arm bracket of the LH side input shaft, and 100 gm weight was placed into the weight pan. The speed for this load was recorded using a tachometer. Also, an additional 100 gm weight was added to the weight pan. The electronic loading cell attached to the output arm bracket was mounted on the load pulley fixed on the RH side output shaft for proper recording. The input and output torque were calculated using arm length = 100 mm. Thus, the observed recording was tabulated, and Torque *versus* speed characteristics and power *versus* speed characteristics were plotted. At the same time, the steps were repeated using varying rope materials such as woolen, cotton, and steel. Finally, the sample was calculated.

Table 2 shows sample calculations for observation

Input Torque	Weight in the pan (N) Input arm length (m) = 0.1 9.81 0.10 0.0981 N-m
Output Torque	Electronic load cell analysis (N)×Length of output arm (m) = 0.170×9.81× 0.1 = 0.1667 N-m
Power consumed across the output shaft	$2\times\pi\times N\times T/60 = 2\times3.143\times2100\times 0.1667 / 60 = 36.656$ Watt
Efficiency	Input / output = 36.656/ 71.56 = 51.23%

The Mechanical Power Amplifier Working Principle

The capstan model, mainly composed of two counter-rotating drums and rope coiled around it, as shown in Fig. 3, serves as the foundation for a mechanical power amplifier's operation.

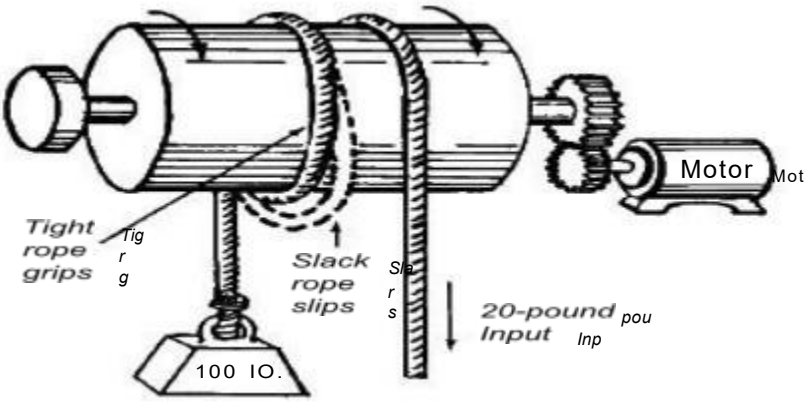

Fig. (3). Basic layout of mechanical power amplifier.

$$T_{load} \square T_{holde} \square\square$$

where T_{laod} is the actual tension on the rope line, T_{hold} is the force that is subsequently applied on the opposite side of the capstan, is the coefficient of friction between the materials of the rope and capstan, and is the total angle swept by all turns of the rope, measured in radians (i.e., with one full turn the angle), as shown in Fig (4). From Fig. 3, it is seen that the gain in force propagates exponentially with the coefficient of friction, the number of turns, and the contact angle. Note that the cylinder radius does not influence the gain in force. Table 3 shows the factor $e^{\mu\varphi}$ based on the number of turns and coefficient of friction.

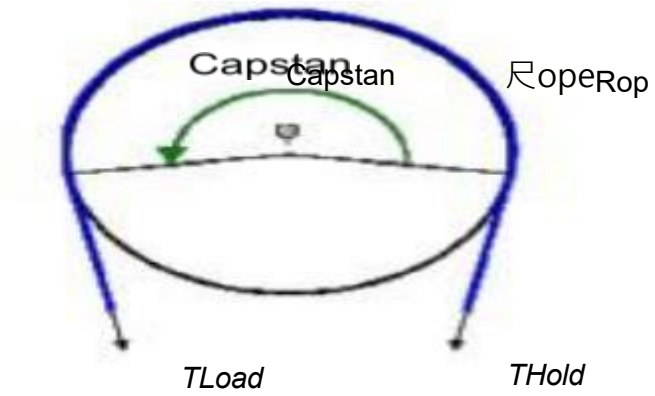

Fig. (4). Working principle of mechanical power amplifier.

Table 3. Capstan Principle.

No of rotation	Coefficient of friction (μ)						
	0.1	**0.2**	**0.3**	**0.4**	**0.5**	**0.6**	**0.7**
1	1.9	3.5	6.6	12	23	43	81
2	3.5	12	43	152	535	1881	6661
3	6.6	43	286	1881	12392	81612	437503
4	12	152	1881	23228	286751	3540026	43702631

Table 3 explains why a sheet, a rope attached to a sail's loose side, rarely wound more than three times around a winch. The force gain would be excessive in addition to being counterproductive because there is a chance of a riding turn, which would cause the sheet to be foul, form a knot, and not run out when relaxed (by letting go of the hold end of the tail, in land-speak). To prevent the rope (anchor warp or sail sheet) from sliding down, it is traditional in ancient and modern worlds for anchor capstans and jib winches to have a somewhat flared-out base instead of being cylindrical. If the rope is tailed (the loose end is pulled clear) by hand or with a self-trailer, it can slowly climb upwards around the winch without much chance of a riding turn. Applying this theory can create a mechanical power amplifier that amplifies the modest control force generated by an input motor. The device's output can then be utilized to demonstrate the implementation of load positioning.

Result and Discussion

The weight pan's input weights were changed over several tests, ranging from 100 g to 1 kg; the electronic load cell's readings variations in the speed, input/output torque, power, and efficiency are documented. Table 6 summarizes the results from utilizing two numbers of turns and rope material as leather. The observations for steel and woven cotton arepresented similarly in Tables 5 and 7. The relationship between speed, torque, power, and efficiency of the power amplifier assembly is displayed below. The findings are strikingly compatible with experimental measurements, including a successful computation of the amplification factor.

Table 4. Loading and unloading data

	Loading		Unloading		Mean Speed(rpm)
	Weight (gm)	Speed rpm	Weight (gm)	Speed (rpm)	
1.	100	2100	100	2100	2100
2.	150	1960	150	1960	1960
3.	200	1750	200	1750	1750
4.	250	1600	250	1600	1600
5.	300	1250	300	1250	1250
6.	350	1050	350	1050	1050
7.	500	810	500	810	810
8.	600	650	600	650	650
9.	700	535	700	535	535
10.	800	520	800	520	520

Table 5. Observation for power amplification factor with steel rope.

S/n	Input load shaft (gm)	Load cell reading at output shaft	Speed (rpm)	Input torque (N-m)	output arm amplified torque	power consumption (watt)	Power amplification factor output/input torque	Efficiency (%)
1	100	110	2100	0.0981	0.10791	23.718618	1.1	33.1439
2	150	180	1960	0.14715	0.17658	36.2247984	1.2	45.17521
3	200	233.3334	1750	0.1962	0.228900065	41.92686198	1.166667	48.7877
4	250	300	1600	0.24525	0.2943	49.28544	1.2	54.11748
5	300	378	1250	0.2943	0.370818	48.515355	1.26	54.81697
6	350	460.83345	1050	0.34335	0.452077614	49.68332983	1.316667	56.629
7	500	614.2855	810	0.4905	0.602614076	51.08962132	1.228571	55.7840
8	600	697.5	650	0.5886	0.6842475	46.55163825	1.1625	51.6985
9	700	882	535	0.6867	0.865242	48.45066786	1.26	54.7756
10	800	1024	520	0.7848	1.004544	54.67398144	1.28	58.9705
11	1000	1290	380	0.981	1.26549	50.3327556	1.29	56.54245

Table 6. Observation for power amplification factor with leather rope.

S/n	Input load shaft (gm)	Load cell reading at output shaft	Speed (rpm)	Input torque (N-m)	output arm amplified torque	power consumption (watt)	Power amplification factor output/input torque	Efficiency (%)
1	100	170	2100	0.0981	0.16677	36.656046	1.7	51.22250825
2	150	262.5	1960	0.14715	0.2575125	52.827831	1.75	65.88051963
3	200	356	1750	0.1962	0.349236	63.968394	1.78	74.43612261
4	250	450	1600	0.24525	0.44145	73.92816	1.8	81.17622256
5	300	540	12500.	2943	0.52974	69.30765	1.8	78.30996817
6	350	647.5	1050	0.34335	0.6351975	69.80820525	1.85	79.56786874
7	500	940	810	0.4905	0.92214	78.1790292	1.88	85.36264583
8	600	1230	650	0.5886	1.20663	82.091061	2.05	91.16729388
9	700	1477	535	0.6867	1.448937	81.13564221	2.11	91.72749805
10	800	1624	520	0.7848	1.593144	86.70951744	2.03	93.52360221
11	1000	2230	380	0.981	2.18763	87.0093372	2.23	97.74392716

Table 7. Observation for power amplification factor with woven cotton rope.

S/n	Input load shaft (gm)	Load cell reading at output shaft	Speed (rpm)	Input torque (N-m)	output arm amplified torque	power consumption (watt)	Power amplification factor output/input torque	Efficiency (%)
1	100	150	2100	0.0981	0.14715	32.34357	1.1	45.19633081
2	150	232.5	1960	0.14715	0.2280825	46.7903646	1.3	58.35131739
3	200	314	1750	0.1962	0.308034	56.421561	1.433333	65.65433287
4	250	400	1600	0.24525	0.3924	65.71392	1.5	72.15664228
5	300	495	1250	0.2943	0.485595	63.5320125	1.6	71.78413748
6	350	588	1050	0.34335	0.576828	63.3933972	1.75	72.25622675
7	500	850	810	0.4905	0.83385	70.693803	1.857143	77.18962655
8	600	1032	650	0.5886	1.012392	68.8764024	1.5625	76.49158315
9	700	1239	535	0.6867	1.215459	68.06165247	1.48	76.94676376
10	800	1472	520	0.7848	1.444032	78.59384832	1.39	84.7701616
11	1000	1850	380	0.981	1.81485	72.182634	1.2	81.08801132

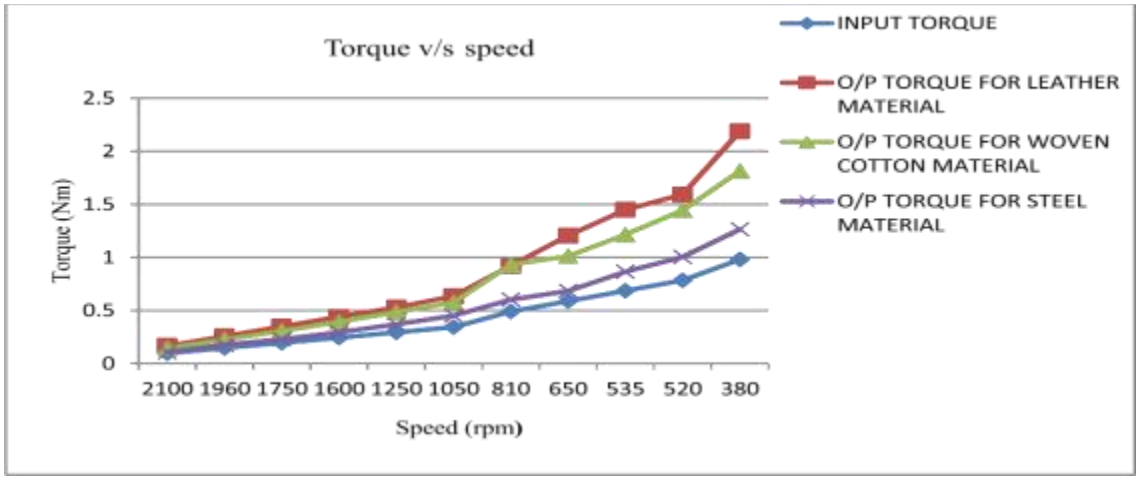

Fig. (5). Torque *versus* speed.

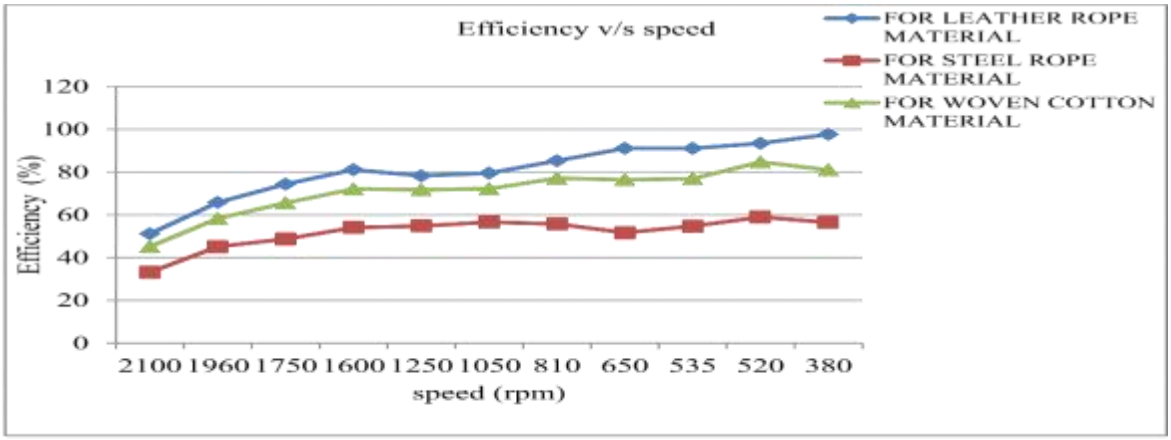

Fig. (6). Efficiency *versus* speed.

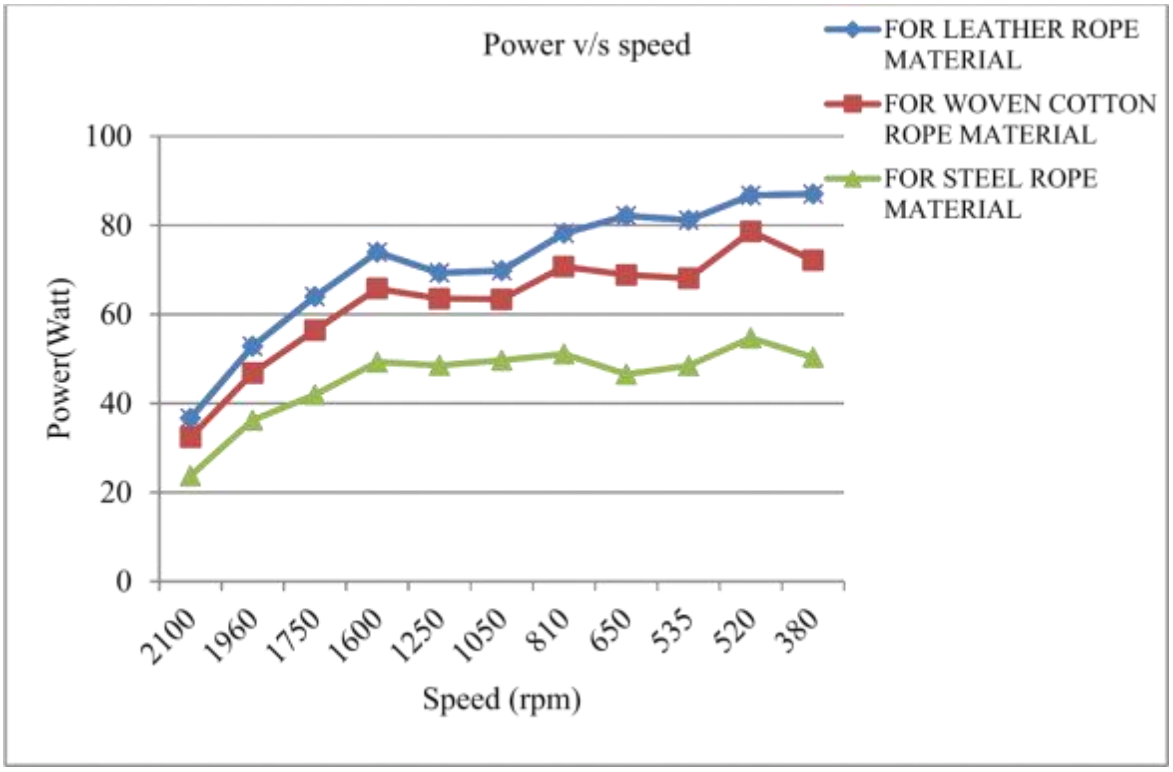

Fig. (7). Power *versus* speed.

It can be noted from Fig. (5) that when the speed decreases, the torque recorded at the input shaft increases due to the increased input load. It is also noted that as the speed decreases, the measured torque at the output shaft increases. The relationship between torque and speed is inverse, although the amplification factor increases as speed drops. The maximum value of the amplification factor is 2.23 for leather rope, 1.867 for woven cotton, and 1.32 for steel at low speeds with correspondingly large torque values. Very little variety remains in the values of the amplification factor. Maximum output torque is attained at 380 revolutions per minute, equaling 2.18 Newton meters for leather, 1.266 Newton meters for steel rope, and 1.815 Newton meters for woven rope.

As shown in Fig. 6, system efficiency rises as speed falls. As a result, efficiency is poor, yet initial speed is high. The efficiency of several power transmission systems, such as the belt drive and gear system, declines as the system's load grows; as a result, the system's total efficiency drops after a certain threshold. At 230 rpm and 1000 g input weight, leather rope material achieves a maximum efficiency of 97.74 percent. Similar to this, woven cotton has a maximum efficiency of 84.87 percent at 520 revolutions per minute and 800 grams. Steel rope material has 520 spins per minute and weighs 800 grams.

As speed decreases, it can be seen from Fig. 7 that power over the system's output shaft increases. As a result, at first, power is low, and speed is high. Power across the output shaft increases when load increases, speed across the shaft decreases, and vice versa. The maximum power at the output arm for leather rope is 87.008 watts, compared to 78.59 watts for woven cotton rope and 54.67 watts for steel. According to experimental studies, a mechanical power amplifier's performance can be improved by raising its amplification factor. The following variable affects the amplifying factor. It is based on the number of rope rotations and the angle at which the rope is wrapped around the capstan drum. The number of turns has an exponential relationship with the amplification factor. However, going beyond two or three spins will result in the rope tangled around the revolving drum, reducing the amount of kinetic energy the drum receives from the electric motor drive. It leads to decreased transmission power and efficiency, producing ludicrous outcomes. Given this, choosing the ideal number of turns, two or three will produce the appropriate outcomes. It also depends on the friction between the rope and the drum. Power amplification can be improved by choosing an elastic rope material with a high coefficient of friction. It is clear that among the other materials, such as woven cotton and steel, the leather-to-steel rope-drum pair has the highest coefficient of friction (0.6).

Conclusion

The primary purpose of this work was to calculate the amplification factor of mechanical power amplifiers for various rope materials such as leather, woven cotton, and steel rope. An intensive combination of analytical and experimental research was utilized to accomplish this goal. The experimental study verifies that maintaining an optimal number of turns equal to two results in a power amplification factor of 2.23 for leather contact, 1.867 for woven cotton contact, and 1.32 for steel contact of rope. This is the case when the optimal number of turns is maintained. It is clear from these results that the power amplification of leather is superior to that of woven cotton and steel. The results showed a remarkable consistency with the experimental measurements, including a positive estimate for the amplification factor.

References

Baser, O., & Ilhan Konukseven, E. (2010). Theoretical and experimental determination of capstan drive slip error. *Mechanism and Machine Theory*, *45*(6). https://doi.org/10.1016/j.mechmachtheory.2009.10.013

Bienert, F., Loescher, A., Röcker, C., Graf, T., & Ahmed, M. A. (2022). Experimental analysis on CPA-free thin-disk multipass amplifiers operated in a helium-rich atmosphere. *Optics Express*, *30*(21). https://doi.org/10.1364/oe.469697

Choi, H. (2023). A Doherty Power Amplifier for Ultrasound Instrumentation. *Sensors*, *23*(5). https://doi.org/10.3390/s23052406

Gawande, S. H. (2018). Performance Evaluation of Mechanical Power Amplifier for Various Belt Materials. *The Open Mechanical Engineering Journal*, *12*(1). https://doi.org/10.2174/1874155x01812010095

Hu, X. Y., Jia, J. H., & Tu, S. T. (2012). Displacement amplifier design for an extensometer in

high-temperature deformation monitoring. *Procedia Engineering*, *29*. https://doi.org/10.1016/j.proeng.2012.01.229

Hu, Y., Yan, Y., Wang, L., & Qian, X. (2016). Non-Contact Vibration Monitoring of Power Transmission Belts Through Electrostatic Sensing. *IEEE Sensors Journal*, *16*(10). https://doi.org/10.1109/JSEN.2016.2530159

Jeong, H., Lee, H. D., Park, B., Jang, S., Kong, S., & Park, C. (2023). Three-Stacked CMOS Power Amplifier to Increase Output Power With Stability Enhancement for mm-Wave Beamforming Systems. *IEEE Transactions on Microwave Theory and Techniques*, *71*(6). https://doi.org/10.1109/TMTT.2022.3228539

Li, K., Li, J. H., Li, L., Zhuo, Y., Pan, B., & Fu, Y. L. (2022). Mechanism synthesis and kinematic analysis of 4-DOF minimally invasive surgical instrument. *Zhejiang Daxue Xuebao (Gongxue Ban)/Journal of Zhejiang University (Engineering Science)*, *56*(6). https://doi.org/10.3785/j.issn.1008-973X.2022.06.008

Paynter, H. M. (2002). The differential analyzer is an active mathematical instrument. *IEEE Control Systems Magazine*, *9*(7). https://doi.org/10.1109/37.41449

Qi, F., Ju, F., Bai, D., Wang, Y., & Chen, B. (2018). Motion modeling and error compensation of a cable-driven continuum robot for applications to minimally invasive surgery. *International Journal of Medical Robotics and Computer Assisted Surgery*, *14*(6). https://doi.org/10.1002/rcs.1932

Schumann, P., Zöllner, R., & Schmidt, T. (2022). A new model and alternative solutions for describing double-layered flexible elements wrapped around a cylinder. *Mechanism and Machine Theory*, *172*. https://doi.org/10.1016/j.mechmachtheory.2022.104823

Shahosseini, I., & Najafi, K. (2014). Mechanical amplifier for translational kinetic energy harvesters. *Journal of Physics: Conference Series*, *557*(1). https://doi.org/10.1088/1742-6596/557/1/012135

Starkey, M. M., & Williams, R. L. (2011). Capstan as a mechanical amplifier. *Proceedings of the ASME Design Engineering Technical Conference*, *6*(PARTS A AND B). https://doi.org/10.1115/DETC2011-48262

Thokale M. J. (2016). Mechanical power amplifier working on a capstan principle. Ijariie. Vol-2 Issue-4

Thomas, G. C., Gimenez, C. C., Chin, E. D., Carmedelle, A. P., & Hoover, A. M. (2012). Controllable, high force amplification using elastic cable capstans. *Proceedings of the ASME Design Engineering Technical Conference*, *4*(PARTS A AND B). https://doi.org/10.1115/DETC2012-71295

Wang, Z., Hu, S., Gu, L., & Lin, L. (2022). Review of Ka-Band Power Amplifier. In *Electronics (Switzerland)* (Vol. 11, Issue 6). https://doi.org/10.3390/electronics11060942